

Article

# Virescenosides from the Holothurian-Associated Fungus *Acremonium striatisporum* Kmm 4401

Olesya I. Zhuravleva <sup>1,2</sup>, Alexandr S. Antonov <sup>1</sup>, Galina K. Oleinikova <sup>1</sup>, Yuliya V. Khudyakova <sup>1</sup>, Roman S. Popov <sup>1</sup>, Vladimir A. Denisenko <sup>1</sup>, Evgeny A. Pislyagin <sup>1</sup> , Ekaterina A. Chingizova <sup>1</sup> and Shamil Sh. Afiyatulloev <sup>1,\*</sup>

<sup>1</sup> G.B. Elyakov Pacific Institute of Bioorganic Chemistry, Far Eastern Branch of the Russian Academy of Sciences, Prospect 100-letiya Vladivostoka, 159, Vladivostok 690022, Russia; zhuravleva.oi@dvvfu.ru (O.I.Z.); pibocfebras@gmail.com (A.S.A.); oleingka@mail.ru (G.K.O.); 161070@rambler.ru (Y.V.K.); prs\_90@mail.ru (R.S.P.); vladenis@pidoc.dvo.ru (V.A.D.); pislyagin@hotmail.com (E.A.P.); martyyas@mail.ru (E.A.C.)

<sup>2</sup> School of Natural Science, Far Eastern Federal University, Sukhanova St., 8, Vladivostok 690000, Russia

\* Correspondence: afiyat@piboc.dvo.ru; Tel.: +7-423-231-1168

Received: 10 October 2019; Accepted: 25 October 2019; Published: 29 October 2019



**Abstract:** Ten new diterpene glycosides virescenosides Z<sub>9</sub>-Z<sub>18</sub> (1–10) together with three known analogues (11–13) and aglycon of virescenoside A (14) were isolated from the marine-derived fungus *Acremonium striatisporum* KMM 4401. These compounds were obtained by cultivating fungus on wort agar medium with the addition of potassium bromide. Structures of the isolated metabolites were established based on spectroscopic methods. The effects of some isolated glycosides and aglycons 15–18 on urease activity and regulation of Reactive Oxygen Species (ROS) and Nitric Oxide (NO) production in macrophages stimulated with lipopolysaccharide (LPC) were evaluated.

**Keywords:** *Acremonium striatisporum*; secondary metabolites; marine fungi; diterpene glycosides; urease activity

## 1. Introduction

Marine fungi are promising and prolific sources of new biologically active compounds. At the same time, glycosylated secondary metabolites of marine fungi such as ribofuranosides, containing as aglycon moieties anthraquinones [1–3], diphenyl ethers [4,5], isocoumarin [6] and naphthyl derivatives [7] are relatively rare. Recently, two steroid glycosides with β-D-mannose as sugar part were isolated from ascomycete *Dichotomomyces cejpai* [8] and new triterpene glycoside auxarthonoside bearing rare sugar N-acetyl-6-methoxy-glucosamine was described from sponge-derived fungus *Auxarthron reticulatum* [9]. Some of these glycosides exhibited cytotoxic [5], radical scavenging [3,4], and neurotropic [8] activities.

During our ongoing search for new natural compounds from marine-derived fungi, we have investigated the strain *Acremonium striatisporum* KMM 4401 associated with the holothurian *Eupentacta fraudatrix*. Twenty-one new diterpene glycosides, virescenosides have previously been isolated from this strain under cultivation on solid rice medium and wort agar medium [10–12]. Virescenosides Z<sub>5</sub> and Z<sub>7</sub> exhibited an unusual 16-chloro-15-hydroxyethyl group as their side chains in aglycones [12]. So, we attempted directed biosynthesis for the production of other halogenated compounds by culturing the fungus *Acremonium striatisporum* KMM 4401 in media containing potassium bromide. Unfortunately, we were unable to obtain glycoside derivatives with the incorporation of a bromine atom in a molecule structure. Chromatographic separation of the CHCl<sub>3</sub>-EtOH extract of the culture of fungus has now led to the isolation of ten undescribed diterpene glycosides virescenosides Z<sub>9</sub>-Z<sub>18</sub>

(1-10) (Figure 1) together with known virescenosides F (11) and G (12), lactone of virescenoside G (13) and aglycon of virescenoside A (14) (Figure S1).

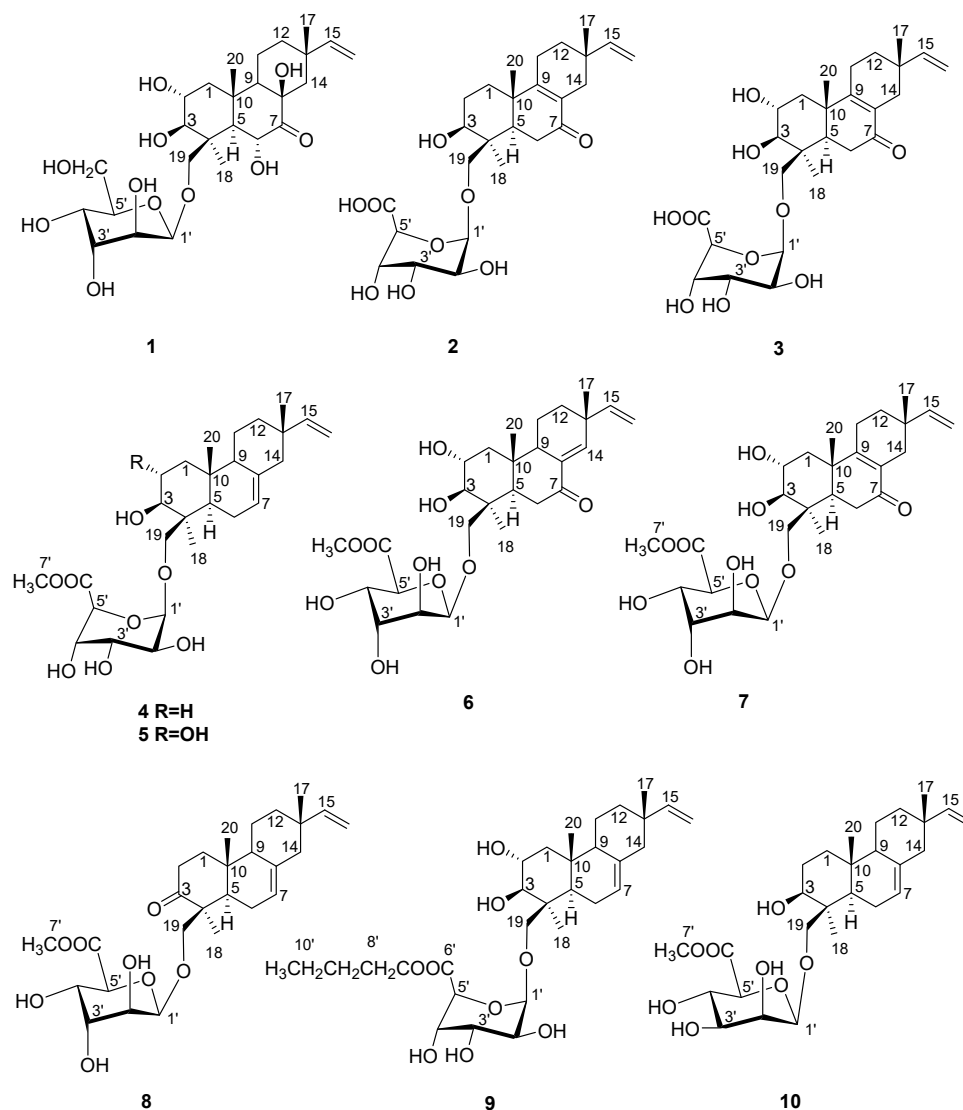


Figure 1. Chemical structures of 1-10.

## 2. Results and Discussion

The  $\text{CHCl}_3$ -EtOH (2:1, v/v) extract of the culture of *A. striatisporum* was separated by low-pressure reversed-phase column chromatography on Teflon powder Polycrome-1 followed by Si gel flash column chromatography and then by RP HPLC to yield individual compounds 1-14 as colorless, amorphous solids.

The molecular formula of virescenoside Z<sub>9</sub> (1) was determined as  $\text{C}_{26}\text{H}_{42}\text{O}_{11}$  based on the analysis of HRESIMS ( $m/z$  529.2656  $[\text{M}-\text{H}]^-$ , calcd for  $\text{C}_{26}\text{H}_{41}\text{O}_{11}$ , 529.2654) and NMR data. A close inspection of the  $^1\text{H}$  and  $^{13}\text{C}$  NMR data (Tables 1 and 2; Figures S3-S8) of 1 by DEPT and HSQC revealed the presence of three quaternary methyls ( $\delta_{\text{H}}$  0.95, 1.28, 1.81;  $\delta_{\text{C}}$  28.5, 17.7, 25.8), six methylenes ( $\delta_{\text{C}}$  18.4, 34.3, 46.9, 49.8, 64.0 and 74.0), including two oxygen-bearing, eight oxygenated methines ( $\delta_{\text{H}}$  3.61, 3.70, 4.28, 4.50, 4.56, 4.69, 4.74, 5.43;  $\delta_{\text{C}}$  84.7, 57.3, 69.1, 75.7, 72.7, 67.2, 72.3, 101.2) including one methine linked to an anomeric carbon, two tertiary ( $\delta_{\text{H}}$  1.93, 2.41;  $\delta_{\text{C}}$  60.5, 55.9), four saturated quaternary carbons ( $\delta_{\text{C}}$  35.8, 43.8 (2C) and 80.2), including one oxygen-bearing, one monosubstituted double bond ( $\delta_{\text{C}}$  108.4, 151.0) and one carbonyl or carboxyl carbon ( $\delta_{\text{C}}$  178.0). HMBC correlations from  $\text{H}_3$ -20 ( $\delta_{\text{H}}$  1.28) to C-1 ( $\delta_{\text{C}}$  46.9), C-5 ( $\delta_{\text{C}}$  55.9), C-9

( $\delta_C$  60.5) and C-10 ( $\delta_C$  43.8), from H<sub>3</sub>-18 ( $\delta_H$  1.81) to C-3 ( $\delta_C$  84.7), C-4 ( $\delta_C$  43.8), C-5 ( $\delta_C$  55.9) and C-19 ( $\delta_C$  74.0), from H-3 ( $\delta_H$  3.61) to C-2 ( $\delta_C$  69.1), C-4 and C-19, from H-1 $\beta$  ( $\delta_H$  2.34) to C-3, from H-6 ( $\delta_H$  3.70) to C-4, C-5, C-7 ( $\delta_C$  178.0) and C-8 ( $\delta_C$  80.2), from H-9 ( $\delta_H$  1.93) to C-8 and C-10 established the structures of the A and B rings and the location of hydroxy groups at C-2, C-3, C-6, C-8 and carbonyl function at C-7. The correlations observed in the COSY and HSQC spectra of **1** indicated the presence of the isolated spin system: >CH-CH<sub>2</sub>-CH<sub>2</sub>- (C-9-C-11-C-12). These data and HMBC correlations from H<sub>3</sub>-17 ( $\delta_H$  0.95) to C-12 ( $\delta_C$  34.3), C-13 ( $\delta_C$  35.8), C-14 ( $\delta_C$  49.8), C-15 ( $\delta_C$  151.0) and from H-14 $\beta$  ( $\delta_H$  1.48) to C-8, C-9 and C-12 established the structure of the C ring in **1**.

The proton signals of a typical ABX system of a vinyl group at  $\delta_H$  6.64 (1H, dd, 10.8, 17.6 Hz), 4.96 (1H, dd, 1.8, 17.6) and 4.85 (1H, dd, 1.8, 10.8) indicated the C-15, C-16 position of this double bond [13–16]. NOE correlations (Figure 2) H<sub>3</sub>-20 ( $\delta_H$  1.28)/H-2 ( $\delta_H$  4.28), H-6 ( $\delta_H$  3.70), H-19b ( $\delta_H$  4.96) and H-5 ( $\delta_H$  2.41)/H-3 ( $\delta_H$  3.62), H<sub>3</sub>-18 ( $\delta_H$  1.81) indicated a *trans*-ring fusion of the A and B rings, as well as the stereochemistry of the methyl and hydroxymethyl groups at C-4, methyl group at C-10 and hydroxy groups at C-2, C-3 and C-6. NOE cross-peaks H-9 ( $\delta_H$  1.93)/H-5 and H-14 $\beta$  ( $\delta_H$  1.48)/H<sub>3</sub>-20, H<sub>3</sub>-17 ( $\delta_H$  0.95), H-6 showed the stereochemistry of the methyl group at C-13 and suggested the  $\beta$ -orientation of hydroxy group at C-8.

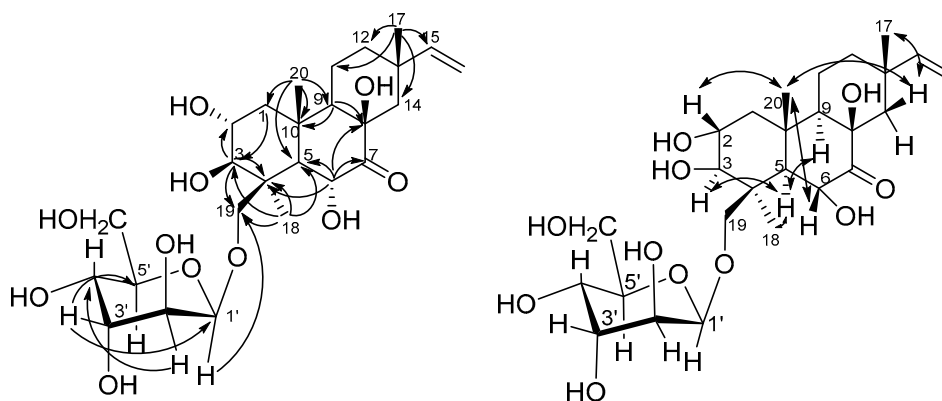


Figure 2. Key HMBC and NOESY correlations of **1**.

Interpretation of the COSY data gave rise to spin systems for monosaccharide involving one anomeric proton, four oxymethines and protons of a hydroxymethyl group. A comparison of the <sup>13</sup>C NMR spectrum of **1** with the data published for  $\alpha$ -D-altropyranoses and  $\beta$ -D-altropyranoses as well as a good coincidence of carbon signals due to the glycosidic moiety with those of virescenosides O, T, W [10] together with magnitudes of <sup>1</sup>H-<sup>1</sup>H spin coupling constants in <sup>1</sup>H NMR spectra of **1** elucidated the presence of a  $\beta$ -D-altropyranoside unit of <sup>4</sup>C<sub>1</sub> form in **1**. A long-range correlation H-1' ( $\delta_H$  5.43)/C-19 as well as the NOESY cross-peak between H-1' and H-19a and downfield chemical shift of C-19 ( $\delta_C$  74.0) revealed a linkage between the altrose and aglycon. Thus, the structure of virescenoside Z<sub>9</sub> (**1**) was represented as 19-O- $\beta$ -D-altropyranosyl-7-oxo-isopimara-15-en-2 $\alpha$ ,3 $\beta$ ,6 $\alpha$ ,8 $\beta$ -tetraol.

In HRESIMS virescenoside Z<sub>10</sub> (**2**) gave a quasimolecular ion at  $m/z$  493.2446 [M-H]<sup>-</sup>. These data, coupled with <sup>13</sup>C NMR spectral data (DEPT), established the molecular formula of **2** as C<sub>26</sub>H<sub>38</sub>O<sub>9</sub>. <sup>1</sup>H and <sup>13</sup>C NMR spectra of **2** (Tables 1 and 2; Figures S9-S13) indicated the presence of a  $\Delta^{15}$ -pimarene-type aglycon possessing primary alcohol on a quaternary carbon (AB system, coupling at 3.73 d, 10.2 Hz and 4.17 d, 10.2 Hz) and one secondary alcohol function at  $\delta_C$  80.0. The remaining functionality, corresponding to the carbon signals at  $\delta$  202.9 (C), 168.7 (C) and 130.3 (C), suggested the presence of the tetrasubstituted enone chromophore. The structure of the aglycon part of **2** was found by extensive NMR spectroscopy to be the same as that of virescenoside P [17].

**Table 1.**  $^{13}\text{C}$  NMR data ( $\delta$  in ppm) for virescenosides Z<sub>9</sub>-Z<sub>18</sub> (1–10).

Position	1 <sup>a</sup>	2 <sup>b</sup>	3 <sup>b</sup>	4 <sup>c</sup>	5 <sup>b</sup>	6 <sup>c</sup>	7 <sup>b</sup>	8 <sup>c</sup>	9 <sup>b</sup>	10 <sup>d</sup>
1	46.9, CH <sub>2</sub>	35.9, CH <sub>2</sub>	44.1, CH <sub>2</sub>	40.0, CH <sub>2</sub>	48.0, CH <sub>2</sub>	46.6, CH <sub>2</sub>	44.1, CH <sub>2</sub>	40.3, CH <sub>2</sub>	48.1, CH <sub>2</sub>	38.5, CH <sub>2</sub>
2	69.1, CH	29.0, CH <sub>2</sub>	69.6, CH	29.4, CH <sub>2</sub>	69.5, CH	69.3, CH	69.4, CH	37.3, CH <sub>2</sub>	69.5, CH	28.6, CH <sub>2</sub>
3	84.7, CH	80.0, CH	84.6, CH	81.5, CH	85.6, CH	84.7, CH	84.4, CH	218.4, C	85.6, CH	79.0, CH
4	43.8, C	41.3, C	44.7, C	43.8, C	44.6, C	44.9, C	44.7, C	54.1, C	44.6, C	43.0, C
5	55.9, CH	51.8, CH	51.7, CH	53.5, CH	53.2, CH	51.9, CH	51.5, CH	55.5, CH	53.2, CH	51.5, CH
6	57.3, CH	37.3, CH <sub>2</sub>	37.6, CH <sub>2</sub>	25.2, CH <sub>2</sub>	25.3, CH <sub>2</sub>	39.3, CH <sub>2</sub>	37.8, CH <sub>2</sub>	25.8, CH <sub>2</sub>	25.3, CH <sub>2</sub>	24.6, CH <sub>2</sub>
7	178.0, C	202.9, C	202.7, C	123.1, CH	123.2, CH	203.1, C	202.8, C	123.1, CH	123.2, CH	122.8, CH
8	80.2, C	130.3, C	130.3, C	137.2, C	137.1, C	136.8, C	130.2, C	137.7, C	136.9, C	134.9, C
9	60.5, CH	168.7, C	167.8, C	54.1, CH	54.1, CH	52.6, CH	167.9, C	53.1, CH	54.1, CH	52.3, CH
10	43.8, C	43.9, C	42.2, C	36.8, C	37.9, C	38.4, C	42.2, C	37.0, C	37.9, C	35.5, C
11	18.4, CH <sub>2</sub>	24.9, CH <sub>2</sub>	25.0, CH <sub>2</sub>	22.1, CH <sub>2</sub>	22.2, CH <sub>2</sub>	21.0, CH <sub>2</sub>	25.0, CH <sub>2</sub>	22.1, CH <sub>2</sub>	22.2, CH <sub>2</sub>	20.5, CH <sub>2</sub>
12	34.3, CH <sub>2</sub>	35.3, CH <sub>2</sub>	35.2, CH <sub>2</sub>	37.9, CH <sub>2</sub>	37.8, CH <sub>2</sub>	35.6, CH <sub>2</sub>	35.2, CH <sub>2</sub>	37.8, CH <sub>2</sub>	37.8, CH <sub>2</sub>	36.4, CH <sub>2</sub>
13	35.8, C	36.0, C	36.1, C	38.4, C	38.4, C	40.4, C	36.1, C	38.4, C	38.4, C	37.1, C
14	49.8, CH <sub>2</sub>	34.9, CH <sub>2</sub>	34.9, CH <sub>2</sub>	47.7, CH <sub>2</sub>	47.6, CH <sub>2</sub>	146.5, CH	34.9, CH <sub>2</sub>	47.6, CH <sub>2</sub>	47.6, CH <sub>2</sub>	46.3, CH <sub>2</sub>
15	151.0, CH	147.0, CH	147.2, CH	152.0, CH	151.9, CH	148.6, CH	146.9, CH	151.9, CH	151.9, CH	150.6, CH
16	108.4, CH <sub>2</sub>	112.7, CH <sub>2</sub>	112.7, CH <sub>2</sub>	110.4, CH <sub>2</sub>	110.4, CH <sub>2</sub>	112.9, CH <sub>2</sub>	112.7, CH <sub>2</sub>	110.5, CH <sub>2</sub>	110.4, CH <sub>2</sub>	109.6, CH <sub>2</sub>
17	28.5, CH <sub>3</sub>	29.2, CH <sub>3</sub>	29.1, CH <sub>3</sub>	22.6, CH <sub>3</sub>	22.6, CH <sub>3</sub>	26.8, CH <sub>3</sub>	29.2, CH <sub>3</sub>	22.6, CH <sub>3</sub>	22.6, CH <sub>3</sub>	21.7, CH <sub>3</sub>
18	25.8, CH <sub>3</sub>	22.8, CH <sub>3</sub>	23.7, CH <sub>3</sub>	23.9, CH <sub>3</sub>	24.6, CH <sub>3</sub>	23.6, CH <sub>3</sub>	23.7, CH <sub>3</sub>	22.0, CH <sub>3</sub>	24.6, CH <sub>3</sub>	23.9, CH <sub>3</sub>
19	74.0, CH <sub>2</sub>	73.3, CH <sub>2</sub>	73.8, CH <sub>2</sub>	73.9, CH <sub>2</sub>	74.1, CH <sub>2</sub>	73.1, CH <sub>2</sub>	73.6, CH <sub>2</sub>	75.1, CH <sub>2</sub>	73.9, CH <sub>2</sub>	72.1, CH <sub>2</sub>
20	17.7, CH <sub>3</sub>	18.7, CH <sub>3</sub>	19.7, CH <sub>3</sub>	16.9, CH <sub>3</sub>	17.6, CH <sub>3</sub>	16.1, CH <sub>3</sub>	19.7, CH <sub>3</sub>	16.7, CH <sub>3</sub>	17.6, CH <sub>3</sub>	15.7, CH <sub>3</sub>
1'	101.2, CH	103.5, CH	103.3, CH	103.7, CH	103.3, CH	102.8, CH	102.8, CH	101.9, CH	103.3, CH	103.5, CH
2'	72.7, CH	71.1, CH	71.3, CH	70.9, CH	71.2, CH	71.6, CH	71.7, CH	72.1, CH	71.3, CH	71.6, CH
3'	72.3, CH	70.8, CH	71.1, CH	70.6, CH	71.1, CH	71.8, CH	72.0, CH	72.0, CH	71.2, CH	75.1, CH
4'	67.2, CH	69.9, CH	69.7, CH	69.9, CH	69.6, CH	69.1, CH	69.0, CH	68.7, CH	69.7, CH	70.0, CH
5'	75.7, CH	76.5, CH	76.6, CH	76.6, CH	76.4, CH	76.4, CH	76.1, CH	76.0, CH	76.4, CH	77.8, CH
6'	64.0, CH <sub>2</sub>	174.0, C	174.0, C	172.7, C	172.9, C	173.2, C	172.8, C	172.6, C	172.9, C	170.7, C
7'				53.3, CH <sub>3</sub>	53.3, CH <sub>3</sub>	53.4, CH <sub>3</sub>	53.3, CH <sub>3</sub>	53.3, CH <sub>3</sub>	66.8, CH <sub>2</sub>	51.8, CH <sub>3</sub>
8'									32.3, CH <sub>2</sub>	
9'									20.7, CH <sub>2</sub>	
10'									14.7, CH <sub>3</sub>	

<sup>a</sup> Chemical shifts were measured at 176.04 in Pyr-d<sub>5</sub>. <sup>b</sup> Chemical shifts were measured at 176.04 in CD<sub>3</sub>OD. <sup>c</sup> Chemical shifts were measured at 125.77 in CD<sub>3</sub>OD. <sup>d</sup> Chemical shifts were measured at 125.77 in Pyr-d<sub>5</sub>.

**Table 2.** <sup>1</sup>H NMR data ( $\delta$  in ppm, *J* in Hz) for virescenosides Z<sub>9</sub>-Z<sub>13</sub> (1–5).

Position	1 <sup>a</sup>	2 <sup>b</sup>	3 <sup>b</sup>	4 <sup>c</sup>	5 <sup>b</sup>
1	$\alpha$ : 1.54 t (11.5) $\beta$ : 2.34 dd (4.6, 12.2)	$\alpha$ : 1.35 m $\beta$ : 1.94 m	$\alpha$ : 1.23 m $\beta$ : 2.17 dd (4.5, 12.8)	$\alpha$ : 1.22 dt (4.6, 13.5) $\beta$ : 1.90 dd (3.5, 13.5)	$\alpha$ : 1.11 $\beta$ : 2.11 dd (4.2, 12.6)
2	4.28 ddd (4.5, 9.3, 11.5)	$\alpha$ : 1.82 dd (3.5, 11.9) $\beta$ : 1.75 dd (4.0, 13.6)	3.82 m	$\alpha$ : 1.74 dd (3.4, 11.8) $\beta$ : 1.65 dd (3.0, 13.4)	3.76 m
3	3.61 d (9.3)	3.26 dd (4.0, 11.9)	2.99 d (9.8)	3.24 dd (4.1, 11.8)	2.98 d (9.8)
5	2.41 d (13.2)	1.67 dd (3.6, 14.4)	1.76 dd (3.5, 14.7)	1.26 t (8.2)	1.34 dd (3.9, 11.4)
6	3.70 d (13.2)	$\alpha$ : 2.54 dd (3.6, 18.0) $\beta$ : 2.64 dd (14.4, 18.0)	$\alpha$ : 2.56 dd (3.3, 18.2) $\beta$ : 2.70 dd (14.7, 18.2)	2.03 m	2.03 m
7				5.38 brs	5.39 brs
9	1.93 t (7.5)			1.66 dd (3.9, 7.8)	1.74 m
11	$\alpha$ : 1.38 m $\beta$ : 1.69 m	$\alpha$ : 2.23 m $\beta$ : 2.27 m	$\alpha$ : 2.26 m $\beta$ : 2.32 m	$\alpha$ : 1.38 m $\beta$ : 1.58 m	$\alpha$ : 1.41 m $\beta$ : 1.61 m
12	$\alpha$ : 1.87 $\beta$ : 1.36	$\alpha$ : 1.35 m $\beta$ : 1.62 m	$\alpha$ : 1.64 m $\beta$ : 1.36 m	$\alpha$ : 1.37 m $\beta$ : 1.48 dt (2.7, 8.9)	$\alpha$ : 1.50 dd (2.8, 12.1) $\beta$ : 1.39 td (2.8, 11.5)
14	$\alpha$ : 2.37 d (14.0) $\beta$ : 1.48 d (14.0)	$\alpha$ : 2.30 d (17.5) $\beta$ : 1.93 d (17.5)	$\alpha$ : 2.31 m $\beta$ : 1.94 dt (2.6, 17.9)	$\alpha$ : 1.97 brd (14.1) $\beta$ : 1.91 dd (2.6, 14.1)	$\alpha$ : 1.99 m $\beta$ : 1.92 dd (2.6, 14.1)
15	6.64 dd (10.8, 17.6)	5.70 dd (10.6, 17.5)	5.70 dd (10.8, 17.5)	5.80 dd (10.7, 17.5)	5.81 dd (10.8, 17.6)
16	a: 4.85 dd (1.8, 10.8) b: 4.96 dd (1.8, 17.6)	a: 4.82 dd (1.4, 17.5) b: 4.93 dd (1.4, 10.6)	a: 4.82 dd (1.5, 17.6) b: 4.93 dd (1.5, 10.8)	a: 4.84 dd (1.3, 10.7) b: 4.92 dd (1.3, 17.5)	a: 4.85 dd (1.4, 10.8) b: 4.93 dd (1.4, 17.6)
17	0.95 s	1.00 s	1.01 s	0.86 s	0.86 s
18	1.81 s	1.13 s	1.16 s	1.10 s	1.11 s
19	a: 4.23 d (9.9) b: 4.98 d (9.9)	a: 3.73 d (10.2) b: 4.17 d (10.2)	a: 3.67 d (10.4) b: 4.14 d (10.4)	a: 3.83 d (10.2) b: 4.04 d (10.2)	a: 3.72 d (10.3) b: 4.03 d (10.3)
20	1.28 s	1.14 s	1.21 s	0.87 s	0.95 s
1	5.43 d (1.2)	4.84 d (2.9)	4.82 d (2.5)	4.85 d (2.5)	4.85 d (2.7)
2'	4.56 dd (1.2, 3.9)	3.77 dd (2.7, 7.8)	3.77 dd (2.5, 7.4)	3.77 dd (2.8, 7.9)	3.77 m
3'	4.74 t (3.7)	3.93 dd (2.9, 7.7)	3.94 dd (3.0, 7.4)	3.89 dd (3.0, 7.9)	3.90 dd (3.3, 7.3)
4'	4.50 m	4.23 t (4.8)	4.20 dd (3.0, 5.7)	4.26 dd (3.0, 4.9)	4.23 dd (3.3, 5.6)
5'	4.69 d (3.2, 12.2)	4.24 d (4.8)	4.22 d (5.7)	4.28 d (4.9)	4.28 d (5.6)
6'	a: 4.40 dd (6.5, 12.3) b: 4.51 m				
7'				3.78 s	3.78 s

<sup>a</sup> Chemical shifts were measured at 700.13 in Pyr-d<sub>5</sub>. <sup>b</sup> Chemical shifts were measured at 700.13 in CD<sub>3</sub>OD. <sup>c</sup> Chemical shifts were measured at 500.13 in CD<sub>3</sub>OD.

The HRESIMS of virescenosides  $Z_{11}$  (**3**) showed the quasimolecular ion at  $m/z$  509.2408  $[M-H]^-$ . These data, coupled with  $^{13}C$  NMR spectral data (DEPT), established the molecular formula of **3** as  $C_{26}H_{38}O_{10}$ . The structure of the aglycon moiety of **3** was found by extensive NMR spectroscopy ( $^1H$ ,  $^{13}C$ , HSQC, HMBC and NOESY) (Tables 1 and 2; Figures S14-S18) to be the same as those of virescenoside M [18].

The  $^{13}C$  and  $^1H$  NMR spectra of the sugar moieties of virescenoside  $Z_{10}$  (**2**) and  $Z_{11}$  (**3**) showed a close similarity of all proton and carbon chemical shifts with those of virescenosides  $Z_7$  and  $Z_8$  [12]. The 7.7-, 7.4-Hz splitting between H-2 and H-3 indicated that both were axial, whereas the 4.8-, 5.7-Hz splitting between H-4 and H-5 showed that these protons in equatorial position. These data and HMBC correlations between anomeric protons and C-5'-methine groups and between H-5' ( $\delta_H$  4.24, 4.22) and C-6' ( $\delta_C$  174.0) suggested the presence of a  $\beta$ -altruronopyranoside unit of  $^1C_4$  conformation in **2** and **3**. The long-range correlations H-1' ( $\delta_H$  4.84, 4.82)/C-19 as well as the NOESY cross-peak between H-1' and H-19a and downfield chemical shifts of C-19 ( $\delta_C$  73.3, 73.8) indicated that sugar moieties were linked at C-19. Earlier in result of reduction of the sum of virescenosides  $Z_4$ - $Z_8$  with  $LiAlH_4$  and the acid hydrolysis of obtained products was isolated D-altrose as the only sugar that was identified by GLC of the corresponding acetylated (+)- and (-)-2-octyl glycosides using authentic samples prepared from D-altrose [12]. Thus, the structure of virescenoside  $Z_{10}$  (**2**) was determined as 19-O- $\beta$ -D-altruronopyranosyl-7-oxo-isopimara-8(9),15-dien-3 $\beta$ -ol, and the structure of virescenoside  $Z_{11}$  (**3**) was established as 19-O- $\beta$ -D-altruronopyranosyl-7-oxo-isopimara-8(9),15-dien-2 $\alpha$ ,3 $\beta$ -diol.

The HRESIMS of virescenosides  $Z_{12}$  (**4**) and  $Z_{13}$  (**5**) showed the quasimolecular ions at  $m/z$  517.2770  $[M + Na]^+$  and  $m/z$  533.2718  $[M + Na]^+$ , respectively. These data, coupled with  $^{13}C$  NMR spectral data (DEPT), established the molecular formula of **4** and **5** as  $C_{27}H_{42}O_8$  and  $C_{27}H_{42}O_9$ , respectively. A close inspection of the  $^1H$  and  $^{13}C$  NMR data of **4** (Tables 1 and 2; Figures S19-S23) revealed that virescenoside  $Z_{12}$  (**4**) was structurally identical to virescenosides B [13] and G [19] (See Extraction and Isolation) with respect to the aglycon. The structure of the aglycon moiety of **5** was found by extensive NMR spectroscopy (Tables 1 and 2; Figures S24-S28) to be the same as that of virescenosides A [13,20] and F [19] (See Extraction and Isolation).

The NMR spectra of glycosides **4** and **5** indicated that both compounds contained closed carbohydrate moieties (Tables 1 and 2). Initial examination of the 1-D proton and one bond correlation NMR data suggested the presence of one sugar (anomeric signals at  $\delta_H$  4.85,  $\delta_C$  103.7 for **4** and  $\delta_H$  4.85,  $\delta_C$  103.3 for **5**). The  $^1H$  and  $^{13}C$  NMR spectra of the sugar parts of **4** and **5** indicated the presence of the methoxy groups (both,  $\delta_H$  3.78,  $\delta_C$  53.3). HMBC correlations from anomeric protons to C5'-methine groups and from H-5' ( $\delta_H$  4.28) to C-6' ( $\delta_C$  172.7, 172.9) and from H<sub>3</sub>-7' ( $\delta_H$  3.78) to C-6' together with magnitudes of  $^1H$ - $^1H$  spin coupling constants suggested the presence of the methyl ester of a  $\beta$ -altruronopyranoside unit of  $^1C_4$  form in **4** and **5**. A long-range correlations H-1' ( $\delta_H$  4.85)/C-19 ( $\delta_C$  73.9, 74.1) as well as the NOESY cross-peaks between H-1' and H-19a ( $\delta_H$  3.83, 3.72) and downfield chemical shifts of C-19 indicated that sugar moieties were linked at C-19. Thus, the structure of virescenoside  $Z_{12}$  (**4**) was determined as 19-O-[(methyl- $\beta$ -D-altruronopyranosyl)-uronat]-isopimara-7,15-dien-3 $\beta$ -ol, and the structure of virescenoside  $Z_{13}$  (**5**) was established as 19-O-[(methyl- $\beta$ -D-altruronopyranosyl)-uronat]-isopimara-7,15-dien-2 $\alpha$ ,3 $\beta$ -diol.

The NMR data (Tables 1 and 3) of virescenosides  $Z_{14}$  (**6**),  $Z_{15}$  (**7**) and  $Z_{16}$  (**8**) suggested the presence of one sugar (anomeric signals at  $\delta_H$  4.78,  $\delta_C$  102.8,  $\delta_H$  4.79,  $\delta_C$  102.8,  $\delta_H$  4.75,  $\delta_C$  101.9). The  $^1H$  and  $^{13}C$  NMR spectra of the sugar moieties of **6**, **7** and **8** showed a close similarity of all proton and carbon chemical shifts and proton multiplicities. These data and HMBC correlations from anomeric protons to C-5' methine groups and from H-5' ( $\delta_H$  4.24, 4.24, 4.23) to C-6' ( $\delta_C$  173.2, 172.8, 172.6) and from H<sub>3</sub>-7' ( $\delta_H$  3.76, 3.76, 3.77) to C-6' suggested the presence of the methyl ester of a  $\beta$ -altruronopyranoside unit in **6**, **7** and **8**. The 7.0-, 7.3-, 8.0-Hz splitting between H-4 and H-5 indicated that both were axial and conformation of sugar parts in **6**, **7** and **8** is  $^4C_1$ .

**Table 3.**  $^1\text{H}$  NMR data ( $\delta$  in ppm,  $J$  in Hz) for virescenosides  $Z_{14}$ - $Z_{18}$  (6–10)

Position	6 <sup>c</sup>	7 <sup>b</sup>	8 <sup>c</sup>	9 <sup>b</sup>	10 <sup>d</sup>
1	$\alpha$ : 1.22 m $\beta$ : 2.07 dd (4.3, 12.7)	$\alpha$ : 1.23 m $\beta$ : 2.18 dd (4.5, 12.8)	$\alpha$ : 1.50 m $\beta$ : 2.19 m	$\alpha$ : 1.11 m $\beta$ : 2.11 dd (4.2, 12.5)	$\alpha$ : 1.15 dt $\beta$ : 1.78 brd (3.9, 13.1)
2	3.79 m	3.80 dd (9.8, 13.9)	$\alpha$ : 2.84 dt (5.4, 14.2) $\beta$ : 2.23 m	3.76 m	$\alpha$ : 1.85 m $\beta$ : 1.92 m
3	3.04 d (9.9)	3.00 d (9.8)		2.98 d (9.8)	3.55 dd (4.0, 11.9)
5	1.73 dd (5.0, 13.8)	1.75 dd (3.4, 14.7)	1.63 dd (4.1, 12.3)	1.34 dd (4.5, 11.8)	1.27 m
6	$\alpha$ : 2.59 dd (5.0, 19.0)	$\alpha$ : 2.53 dd (3.4, 18.2) $\beta$ : 2.80 dd (14.7, 18.2)	$\alpha$ : 2.04 m $\beta$ : 2.11 m	$\alpha$ : 2.01 m $\beta$ : 2.06 m	$\alpha$ : 2.06 m $\beta$ : 2.40 m
7			5.41 brs	5.38 m	5.30 m
9	2.13 m		1.76 m	1.74 m	1.60 m
11	$\alpha$ : 1.79 m $\beta$ : 1.54 m	$\alpha$ : 2.26 m $\beta$ : 2.31 m	$\alpha$ : 1.64 m $\beta$ : 1.47 m	$\alpha$ : 1.41 m $\beta$ : 1.61 m	$\alpha$ : 1.46 m $\beta$ : 1.32 m
12	$\alpha$ : 1.54 m $\beta$ : 1.67 m	$\alpha$ : 1.64 m $\beta$ : 1.36 m	$\alpha$ : 1.51 $\beta$ : 1.44	$\alpha$ : 1.50 m $\beta$ : 1.39 m	$\alpha$ : 1.32 m $\beta$ : 1.45 m
14	6.68 t (2.1)	$\alpha$ : 2.32 m $\beta$ : 1.95 d (17.8)	$\alpha$ : 2.00 m $\beta$ : 1.94 d (2.6, 14.0)	$\alpha$ : 1.99 m $\beta$ : 1.92 dd (2.6, 14.1)	$\alpha$ : 2.03 brd (14.0) $\beta$ : 1.94 brd (14.0)
15	5.83 dd (10.7, 17.5)	5.71 dd (10.8, 17.5)	5.81 dd (10.7, 17.5)	5.81 dd (10.8, 17.4)	5.87 dd (10.6, 17.4)
16	5.00 m	a: 4.83 dd (1.2, 17.5) b: 4.93 dd (1.2, 10.8)	a: 4.86 dd (1.4, 10.7) b: 4.94 dd (1.4, 17.5)	a: 4.85 dd (1.4, 10.8) b: 4.93 dd (1.4, 17.4)	a: 4.95 d (10.6) b: 5.02 d (17.4)
17	1.12 s	1.01 s	0.89 s	0.86 s	0.90 s
18	1.13 s	1.15 s	1.11 s	1.11 s	1.41 s
19	a: 3.68 d (10.3) b: 4.09 d (10.3)	a: 3.65 d (10.4) b: 4.11 d (10.4)	a: 3.90 d (9.8) b: 3.96 d (9.8)	a: 3.71 d (10.5) b: 4.04 d (10.53)	a: 4.26 d (10.3) b: 4.59 d (10.3)
20	0.95 s	1.22 s	1.17 s	0.95 s	0.93 s
1'	4.78 brs	4.79 d (2.0)	4.75 d (1.9)	4.84 d (2.1)	4.97 brs
2'	3.76 m	3.76 m	3.66 dd (1.9, 5.6)	3.77 dd (2.5, 7.4)	4.55 d (3.2)
3'	3.91 dd (3.3, 6.3)	3.92 dd (3.3, 6.0)	3.89 dd (3.0, 5.6)	3.92 dd (3.0, 7.4)	4.14 dd (3.3, 9.4)
4'	4.15 dd (3.3, 7.0)	4.14 dd (3.3, 7.3)	4.08 dd (3.2, 8.0)	4.22 m	4.87 t (9.3)
5'	4.24 d (7.0)	4.24 d (7.3)	4.23 d (8.0)	4.25 d (5.6)	4.40 d (9.3)
7'	3.76 s	3.76 s	3.77 s	a: 4.15 dt (6.6, 10.7) b: 4.19 m	3.64 s
8'				a,b: 1.68 m	
9'				a,b: 1.45 m	
10'				0.96 t (7.5)	

<sup>a</sup> Chemical shifts were measured at 700.13 in Pyr-d<sub>5</sub>. <sup>b</sup> Chemical shifts were measured at 700.13 in CD<sub>3</sub>OD. <sup>c</sup> Chemical shifts were measured at 500.13 in CD<sub>3</sub>OD. <sup>d</sup> Chemical shifts were measured at 500.13 in Pyr-d<sub>5</sub>.

The HRESIMS of virescenosides **Z**<sub>14</sub> (**6**) showed the quasimolecular ion at  $m/z$  547.2508 [M + Na]<sup>+</sup>. These data, coupled with <sup>13</sup>C NMR spectral data (DEPT), established the molecular formula of **6** as C<sub>27</sub>H<sub>40</sub>O<sub>10</sub>. The structure of the aglycon moiety of **6** was found by extensive NMR spectroscopy (<sup>1</sup>H, <sup>13</sup>C, HSQC, HMBC and NOESY) (Tables 1 and 3; Figures S29-S33) to be the same as those of virescenoside V [21].

The molecular formula of virescenoside **Z**<sub>15</sub> (**7**) was determined as C<sub>27</sub>H<sub>40</sub>O<sub>10</sub> based on the analysis of HRESIMS ( $m/z$  523.2550 [M-H]<sup>-</sup>, calcd for C<sub>27</sub>H<sub>39</sub>O<sub>10</sub>, 523.2549) and NMR data. The <sup>1</sup>H and <sup>13</sup>C NMR data (Tables 1 and 3; Figures S34-S38) observed for the aglycon part of **7** closely resembled those obtained for virescenoside **Z**<sub>10</sub> (**2**) with the exception of the C-1-C-4 carbon and proton signals of ring A. The HMBC correlations from H-5 ( $\delta_H$  1.75) to C-3 ( $\delta_C$  84.4), H-3 ( $\delta_H$  3.00) and from H<sub>2</sub>-1 ( $\delta_H$  1.23, 2.18) to C-2 ( $\delta_C$  69.2) and downfield chemical shifts of C-2 placed an additional hydroxy group at C-2 of ring A. The relative stereochemistry of protons on C-2 and C-3 was defined based on the <sup>1</sup>H-<sup>1</sup>H coupling constant ( $J=9.8$ ) and assigned as axial. Previously, a similar aglycon has been described for virescenoside M [10].

The HRESIMS of virescenoside **Z**<sub>16</sub> (**8**) showed the quasimolecular at  $m/z$  515.2617 [M + Na]<sup>+</sup>. These data, coupled with <sup>13</sup>C NMR spectral data (DEPT), established the molecular formula of **8** as C<sub>27</sub>H<sub>40</sub>O<sub>8</sub> (Tables 1 and 3). The structure of the aglycon moiety of **8** was found by 2D NMR experiments (Figures S39-S43) to be the same as that of virescenoside **Z**<sub>4</sub> [12].

The attachment of a carbohydrate chains at C-19 of aglycon moieties of **6**, **7** and **8** was confirmed by cross-peaks H-1' ( $\delta_H$  4.78, 4.79, 4.75)/H-19a ( $\delta_H$  3.68, 3.65, 3.90) and H-1'/C-19 ( $\delta_C$  73.1, 73.6, 75.1) in the NOESY and HMBC spectra, respectively. From all these data, virescenoside **Z**<sub>14</sub> (**6**) was structurally identified as 19-O-[(methyl- $\beta$ -D-altruronopyranosyl)-uronat]-7-oxo-isopimara-8(14),15-dien-2 $\alpha$ ,3 $\beta$ -diol, virescenoside **Z**<sub>15</sub> (**7**) as 19-O-[(methyl- $\beta$ -D-altruronopyranosyl)-uronat]-7-oxo-isopimara-8(9),15-dien-2 $\alpha$ ,3 $\beta$ -diol and virescenoside **Z**<sub>16</sub> (**8**) as 19-O-[(methyl- $\beta$ -D-altruronopyranosyl)-uronat]-3-oxo-isopimara-7,15-dien.

The HRESIMS of virescenoside **Z**<sub>17</sub> (**9**) showed the quasimolecular ion at  $m/z$  575.3194 [M + Na]<sup>+</sup>. These data, coupled with <sup>13</sup>C NMR spectral data (DEPT), established the molecular formula of **9** as C<sub>30</sub>H<sub>48</sub>O<sub>9</sub>. The <sup>1</sup>H and <sup>13</sup>C NMR data observed for aglycon and sugar (C-1'-C-6') parts of **9** (Tables 1 and 3; Figures S44-S48) matched those reported for virescenoside **Z**<sub>13</sub> (**5**). The correlations observed in the COSY and HSQC spectra of **9** indicated the presence of the isolated spin system: -CH<sub>2</sub>-CH<sub>2</sub>-CH<sub>2</sub>-CH<sub>3</sub> (C-7'-C-10'). These data and HMBC correlations from H<sub>3</sub>-10' ( $\delta_H$  0.96) to C-8' ( $\delta_C$  32.3), C-9' ( $\delta_C$  20.7) and from Ha-7' ( $\delta_H$  4.15) to C-6' ( $\delta_C$  172.9), C-8' and C-9' suggested the presence of the butyl ester of a  $\beta$ -altruronopyranoside unit of <sup>1</sup>C<sub>4</sub> form in **9**. On the basis of all the data above, the structure of virescenosides **Z**<sub>17</sub> (**9**) was established as 19-O-[(butyl- $\beta$ -D-altruronopyranosyl)-uronat]-isopimara-7,15-dien-2 $\alpha$ ,3 $\beta$ -diol.

The HRESIMS of virescenoside **Z**<sub>18</sub> (**10**) showed the quasimolecular at  $m/z$  517.2773 [M + Na]<sup>+</sup>. These data, coupled with <sup>13</sup>C NMR spectral data (DEPT), established the molecular formula of **10** as C<sub>27</sub>H<sub>42</sub>O<sub>8</sub>. The <sup>1</sup>H and <sup>13</sup>C NMR data observed for the aglycon part of **10** (Tables 1 and 3; Figures S49-S54) matched those reported for virescenoside Q [17]. Initial examination of the 1-D proton and one bond correlation NMR data suggested the presence of one sugar (anomeric signal at  $\delta_H$  4.97,  $\delta_C$  103.5). The <sup>1</sup>H and <sup>13</sup>C NMR spectra of the sugar part of **10** indicated the presence of the methoxycarbonyl group ( $\delta_H$  3.64,  $\delta_C$  51.8, 170.7). A comparison of the <sup>13</sup>C NMR spectrum with the data published for  $\alpha$ - and  $\beta$ -D-mannopyranoses as well as a good coincidence of carbon signals C-1'-C-4' with those of virescenoside Q together with magnitudes of <sup>1</sup>H-<sup>1</sup>H spin coupling constants in <sup>1</sup>H NMR spectrum of **10** elucidated the presence of  $\beta$ -D-mannouronopyranoside unit of <sup>4</sup>C<sub>1</sub> form in **10** [17,22,23]. A long-range correlation H-1' ( $\delta_H$  4.97)/C-19 ( $\delta_C$  72.1) as well as the NOESY cross-peak between H-1' and H-19a ( $\delta_H$  4.26) and downfield chemical shifts of C-19 indicated that sugar moiety was linked at C-19. Thus, the structure of virescenoside **Z**<sub>18</sub> (**10**) was determined as 19-O-[(methyl- $\beta$ -D-mannopyranosyl)-uronat]-isopimara-7,15-dien-3 $\beta$ -ol.

Since methanol is used in the isolation procedure of virescenosides, it is possible that the methyl esters of the sugar units may be obtained during the course of isolation. Therefore, we separated the part of subfraction II by RP-HPLC using acetonitrile instead of methanol and obtain virescenosides Z<sub>12</sub> (4) and Z<sub>13</sub> (5) which were characterized by <sup>1</sup>H and <sup>13</sup>C NMR spectra. Furthermore, we observed compounds 4–8 and 10 in subfraction II by HPLC-MS method (See Supplementary Figure S2).

The structures of known compounds virescenosides F (11) and G (12), lactone of virescenoside G (13) [19] and aglycon of virescenoside A (14) [13] (See Supplementary Figure S1) were determined based on HRESIMS and NMR data and comparison with literature. The aglycons of virescenosides B (15, 16), C (17) and M (18) (See Supplementary Figure S1, Experimental Section) were prepared as a result of acid hydrolysis of the corresponding glycosides for examination of their biological activity.

Next, we investigated the effects of some isolated compounds and aglycons 15–18 on urease activity and regulation of ROS and NO production in macrophages stimulated with lipopolysaccharide (LPS).

The development of urease inhibitors, usually considered as antiulcer agents, carries a significant interest for medicinal chemists. Urease is an enzyme that is clinically used as diagnostic to determine the presence of pathogens in the gastrointestinal and urinary tracts. It has been described that the bacterial urease causes many clinically harmful infections, like stomach cancer, infectious stones and peptic ulcer formation in human and animal health [24]. Urease is also involved in the pathogenesis of hepatic coma, urolithiasis, urinary catheter encrustation and oral cavity infections by hydrolyzing the salivary urea [25].

Aglycons 14 and 15 inhibit urease activity with an IC<sub>50</sub> of 138.8 and 125.0 μM, respectively. Thiourea used as positive control inhibited urease activity with IC<sub>50</sub> of 23.0 μM.

Compounds 1, 2, 5, 15–18 at a concentration of 10 μM induced a significant down-regulation of ROS production in macrophages stimulated with lipopolysaccharide (LPS) (Figure 3). Virescenoside Z<sub>10</sub> (2) decreased the ROS content in macrophages by 45%.

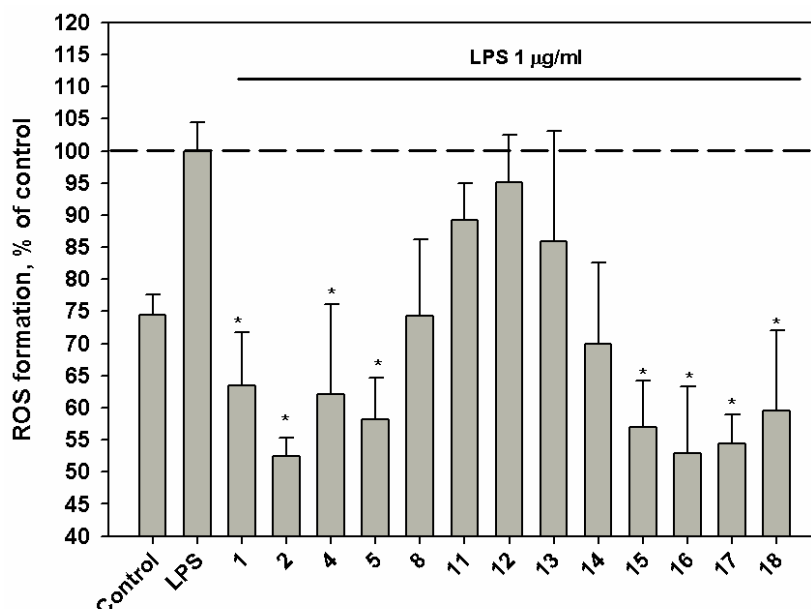


**Figure 3.** Influence of compounds upon ROS level in murine peritoneal macrophages, co-incubated with LPS from *E. coli*. The compounds were tested at a concentration of 10 μM. Time of cell incubation with compounds was 1 h at 37 °C. \* p < 0.05.

Compounds 2, 5, 16 and 17 induced a moderate down-regulation of NO production in LPS-stimulated macrophages at concentration of 1 μM (Figure 4).

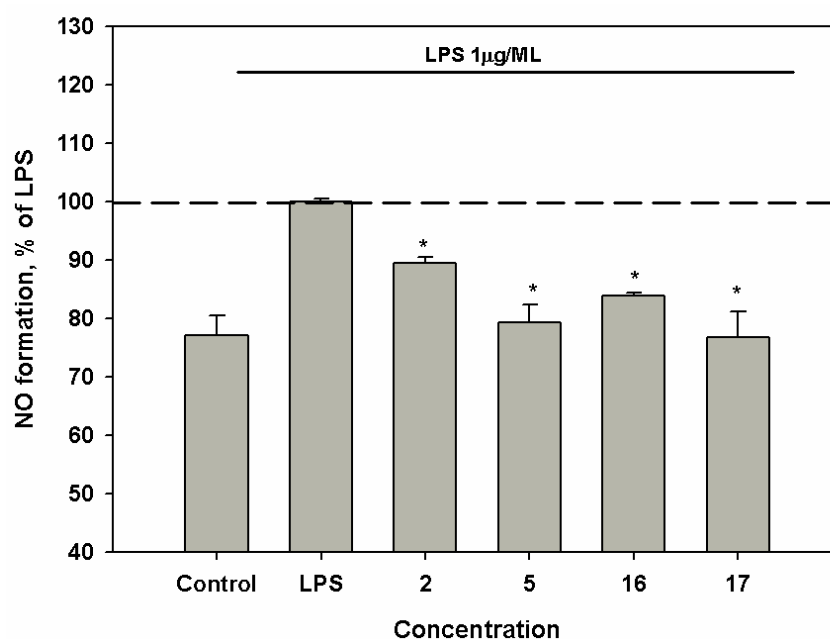


**Figure 4.** Influence of compounds upon RNS level in murine peritoneal macrophages, co-incubated with LPS from *E. coli*. The compounds were tested at a concentration of 1  $\mu$ M. Time of cell incubation with compounds was 1 h at 37 °C. \*  $p < 0.05$ .

### 3. Materials and Methods

#### 3.1. General Experimental Procedures

Optical rotations were measured on a Perkin-Elmer 343 polarimeter (Perkin Elmer, Waltham, MA, USA). UV spectra were recorded on a Shimadzu UV-1601PC spectrometer (Shimadzu Corporation, Kyoto, Japan) in methanol. NMR spectra were recorded in  $CD_3OD$ ,  $CDCl_3$ ,  $DMSO-d_6$  and  $C_5D_5N$  on a Bruker DPX-500 (Bruker BioSpin GmbH, Rheinstetten, Germany) and a Bruker DRX-700 (Bruker BioSpin GmbH, Rheinstetten, Germany) spectrometer, using TMS as an internal standard. The Bruker Impact II Q-TOF mass spectrometer (Bruker Daltonics, Bremen, Germany) was used to record the MS and MS/MS spectra within  $m/z$  range 50–1500. The capillary voltage was set to 1300 V, and the drying gas was heated to 150 °C at the flow rate 3 L/min. Collision-induced dissociation (CID) product ion mass spectra were obtained using nitrogen as the collision gas. The instrument was operated using the program otofControl (ver. 4.0, Bruker Daltonics, Bremen, Germany) and the data were analyzed using the DataAnalysis Software (ver. 4.3, Bruker Daltonics, Bremen, Germany).

Low-pressure liquid column chromatography was performed using silica gel (50/100  $\mu$ m, Imid, Russia) and Polychrome-1 (powder Teflon, Biolar, Latvia). Plates precoated with silica gel (5–17  $\mu$ m, 4.5  $\times$  6.0 cm, Imid) and silica gel 60 RP-18 F<sub>254</sub>S (20  $\times$  20 cm, Merck KGaA, Germany) were used for thin-layer chromatography. Preparative HPLC was carried out on a Agilent 1100 chromatography (Agilent Technologies, USA) using a YMC ODS-AM (YMC Co., Ishikawa, Japan) (5  $\mu$ m, 10  $\times$  250 mm) and YMC ODS-A (YMC Co., Ishikawa, Japan) (5  $\mu$ m, 4.6  $\times$  250 mm) columns with a Agilent 1100 refractometer (Agilent Technologies, USA).

#### 3.2. Cultivation of Fungus

The fungus was grown stationary at 22 °C for 14 days on 6 flasks (1 L) (medium: wort-200 mL, sodium tartrate-0.05 g/L, agar-20 g/L, potassium bromide-30 g/L, seawater-800 mL).

### 3.3. Extraction and Isolation

At the end of the incubation period, the mycelium and medium were homogenized and extracted three times with a mixture of  $\text{CHCl}_3$ –EtOH (2:1, v/v, 2.5 L). The combined extracts (4.5 g) were concentrated to dryness and separated by low pressure RP CC (the column  $20 \times 8$  cm) on Polychrome-1 Teflon powder in  $\text{H}_2\text{O}$  and 50% EtOH. After elution of inorganic salts and highly polar compounds by  $\text{H}_2\text{O}$ , 50% EtOH was used to obtain the fraction of amphiphilic compounds, including the virescenosides. After evaporation of the solvent, the residual material (2.6 g) was subjected to Si gel flash CC ( $7 \times 13$  cm) chromatography with a solvent gradient system of increasing polarity from 10 to 60% EtOH in  $\text{CHCl}_3$  (total volume 8 L). Fractions of 20 mL were collected and combined by TLC examination to obtain two subfractions. Subfraction I ( $\text{CHCl}_3$ –EtOH 5:1, 3:1, 180 mg) was purified and separated by RP HPLC on a YMC ODS-A column eluting with MeOH– $\text{H}_2\text{O}$ –TFA (85:15:0.1) to yield **8** (2.4 mg), **9** (3.6 mg), **13** (2.4 mg) and **14** (4.0 mg). Subfraction II ( $\text{CHCl}_3$ –EtOH 2:1, 840 mg) was purified by RP HPLC on a YMC ODS-AM column eluting at first with MeOH– $\text{H}_2\text{O}$ –TFA (80:20:0.1) and then with MeOH– $\text{H}_2\text{O}$ –TFA (70:30:0.1) to yield **1** (2.5 mg), **2** (2.5 mg), **3** (7.5 mg), **4** (15.5 mg), **5** (71 mg), **6** (1.4 mg), **7** (6.6 mg) **10** (1.4 mg), **11** (98 mg) and **12** (63 mg).

The part of subfraction II (35 mg) was purified by RP HPLC on a YMC ODS-A column eluting with  $\text{CH}_3\text{CN}$ – $\text{H}_2\text{O}$ –TFA (50:50:0.1) to yield **4** (1.1 mg), **5** (4.5 mg), **11** (6 mg) and **12** (2 mg).

### 3.4. Spectral Data

Virescenoside **Z<sub>9</sub>** (**1**): amorphous solids;  $[\alpha]_{\text{D}}^{20} +1.5$  (*c* 0.15, MeOH);  $^1\text{H}$  and  $^{13}\text{C}$  NMR data, see Tables 1 and 2, Supplementary Figures S3–S8; HRESIMS *m/z* 553.2618  $[\text{M} + \text{Na}]^+$  (calcd. for  $\text{C}_{26}\text{H}_{42}\text{O}_{11}\text{Na}$ , 553.2619,  $\Delta + 0.2$  ppm).

Virescenoside **Z<sub>10</sub>** (**2**): amorphous solids;  $[\alpha]_{\text{D}}^{20} +10.0$  (*c* 0.09, MeOH); UV (MeOH)  $\lambda_{\text{max}}$  ( $\log \epsilon$ ) 248 (3.91) nm;  $^1\text{H}$  and  $^{13}\text{C}$  NMR data, see Tables 1 and 2, Supplementary Figures S9–S13; HRESIMS *m/z* 493.2446  $[\text{M} - \text{H}]^-$  (calcd. for  $\text{C}_{26}\text{H}_{37}\text{O}_9$ , 493.2443,  $\Delta -0.6$  ppm).

Virescenoside **Z<sub>11</sub>** (**3**): amorphous solids;  $[\alpha]_{\text{D}}^{20} +7.5$  (*c* 0.10, MeOH); UV (MeOH)  $\lambda_{\text{max}}$  ( $\log \epsilon$ ) 248 (3.64) nm;  $^1\text{H}$  and  $^{13}\text{C}$  NMR data, see Tables 1 and 2, Supplementary Figures S14–S18; HRESIMS *m/z* 509.2403  $[\text{M} - \text{H}]^-$  (calcd. for  $\text{C}_{26}\text{H}_{37}\text{O}_{10}$ , 509.2392,  $\Delta -2.0$  ppm).

Virescenoside **Z<sub>12</sub>** (**4**): amorphous solids;  $[\alpha]_{\text{D}}^{20} -50.0$  (*c* 0.10, MeOH);  $^1\text{H}$  and  $^{13}\text{C}$  NMR data, see Tables 1 and 2, Supplementary Figures S19–S23; HRESIMS *m/z* 517.2770  $[\text{M} + \text{Na}]^+$  (calcd. for  $\text{C}_{27}\text{H}_{42}\text{O}_8\text{Na}$ , 517.2772,  $\Delta + 0.4$  ppm).

Virescenoside **Z<sub>13</sub>** (**5**): amorphous solids;  $[\alpha]_{\text{D}}^{20} -69.2$  (*c* 0.13, MeOH);  $^1\text{H}$  and  $^{13}\text{C}$  NMR data, see Tables 1 and 2, Supplementary Figures S24–S28; HRESIMS *m/z* 533.2718  $[\text{M} + \text{Na}]^+$  (calcd. for  $\text{C}_{27}\text{H}_{42}\text{O}_9\text{Na}$ , 533.2721,  $\Delta + 0.6$  ppm).

Virescenoside **Z<sub>14</sub>** (**6**): amorphous solids;  $[\alpha]_{\text{D}}^{20} -44.0$  (*c* 0.10, MeOH); UV (MeOH)  $\lambda_{\text{max}}$  ( $\log \epsilon$ ) 249 (3.81) nm;  $^1\text{H}$  and  $^{13}\text{C}$  NMR data, see Tables 1 and 3, Supplementary Figures S29–S33; HRESIMS *m/z* 547.2508  $[\text{M} + \text{Na}]^+$  (calcd. for  $\text{C}_{27}\text{H}_{40}\text{O}_{10}\text{Na}$ , 547.2514,  $\Delta +1.0$  ppm).

Virescenoside **Z<sub>15</sub>** (**7**): amorphous solids;  $[\alpha]_{\text{D}}^{20} +17.3$  (*c* 0.15, MeOH); UV (MeOH)  $\lambda_{\text{max}}$  ( $\log \epsilon$ ) 248 (3.99) nm;  $^1\text{H}$  and  $^{13}\text{C}$  NMR data, see Tables 1 and 3, Supplementary Figures S34–S38; HRESIMS *m/z* 547.2515  $[\text{M} + \text{Na}]^+$  (calcd. for  $\text{C}_{27}\text{H}_{40}\text{O}_{10}\text{Na}$ , 547.2514,  $\Delta -0.2$  ppm).

Virescenoside **Z<sub>16</sub>** (**8**): amorphous solids;  $[\alpha]_{\text{D}}^{20} -78.0$  (*c* 0.05, MeOH);  $^1\text{H}$  and  $^{13}\text{C}$  NMR data, see Tables 1 and 3, Supplementary Figures S39–S43; HRESIMS *m/z* 515.2617  $[\text{M} + \text{Na}]^+$  (calcd. for  $\text{C}_{27}\text{H}_{40}\text{O}_8\text{Na}$ , 515.2615,  $\Delta -0.4$  ppm).

Virescenoside **Z<sub>17</sub>** (**9**): amorphous solids;  $[\alpha]_{\text{D}}^{20} -60.0$  (*c* 0.10, MeOH);  $^1\text{H}$  and  $^{13}\text{C}$  NMR data, see Tables 1 and 3, Supplementary Figures S44–S48; HRESIMS *m/z* 575.3194  $[\text{M} + \text{Na}]^+$  (calcd. for  $\text{C}_{29}\text{H}_{48}\text{O}_9\text{Na}$ , 575.3191,  $\Delta -0.5$  ppm), *m/z* 551.3229  $[\text{M} - \text{H}]^-$  calcd. for  $\text{C}_{29}\text{H}_{47}\text{O}_9$ , 551.3226,  $\Delta -0.6$  ppm).

Virescenoside **Z<sub>18</sub>** (**10**): amorphous solids;  $[\alpha]_{\text{D}}^{20} -32.5$  (*c* 0.12, MeOH);  $^1\text{H}$  and  $^{13}\text{C}$  NMR data, see Tables 1 and 3, Supplementary Figures S49–S54; HRESIMS *m/z* 517.2773  $[\text{M} + \text{Na}]^+$  (calcd. for  $\text{C}_{27}\text{H}_{42}\text{O}_8\text{Na}$ , 517.2772,  $\Delta -0.3$  ppm).

Virescenoside F (**11**): amorphous solids;  $^1\text{H}$  NMR (700 MHz,  $\text{CD}_3\text{OD}$ )  $\delta$ : 5.80 (1H, dd,  $J = 10.8, 17.4$  Hz, H-15), 5.38 (1H, m, H-7), 4.92 (1H, dd,  $J = 1.4, 17.4$  Hz, H-16b), 4.86 (1H, d,  $J = 3.0$  Hz, H-1'), 4.85 (1H, dd,  $J = 1.4, 10.8$  Hz, H-16a), 4.27 (1H, t,  $J = 3.7$  Hz, H-4'), 4.24 (1H, d,  $J = 4.3$  Hz, H-5'), 4.12 (1H, d,  $J = 9.8$  Hz, H-19b), 3.93 (1H, dd,  $J = 3.3, 8.3$  Hz, H-3'), 3.78 (1H, dd,  $J = 3.0, 8.0$  Hz, H-2'), 3.76 (1H, m, H-2), 3.73 (1H, d,  $J = 9.8$  Hz, H-19a), 2.98 (1H, d,  $J = 9.8$  Hz, H-3), 2.11 (1H, dd,  $J = 4.2, 12.5$  Hz, H-1 $\beta$ ), 2.04 (1H, m, H-2-6), 1.99 (1H, m, H-14 $\alpha$ ), 1.92 (1H, dd,  $J = 2.8, 14.4$  Hz, H-14 $\beta$ ), 1.73 (1H, m, H-9), 1.60 (1H, m, H-11 $\alpha$ ), 1.50 (1H, m, H-12 $\alpha$ ), 1.39 (1H, m, H-12 $\beta$ ), 1.39 (1H, m, H-11 $\beta$ ), 1.34 (1H, dd,  $J = 5.8, 10.7$  Hz, H-5), 1.14 (3H, s, Me-18), 1.11 (1H, d,  $J = 12.3$  Hz, H-1 $\alpha$ ), 0.92 (3H, s, Me-20), 0.86 (3H, s, Me-17).  $^{13}\text{C}$  NMR (176 MHz,  $\text{CD}_3\text{OD}$ )  $\delta$ : 174.0 (C-6'), 151.9 (C-15), 136.9 (C-8), 123.2 (C-7), 110.4 (C-16), 103.5 (C-1'), 85.8 (C-3), 76.6 (C-5'), 74.3 (C-19), 70.9 (C-2'), 70.4 (C-3'), 70.2 (C-4'), 69.7 (C-2), 54.1 (C-9), 53.4 (C-5), 48.0 (C-1), 47.6 (C-14), 44.4 (C-4), 38.4 (C-13), 37.9 (C-10), 37.9 (C-12), 25.1 (C-6), 24.2 (C-18), 22.6 (C-17), 22.1 (C-11), 17.7 (C-20); Supplementary Figures S55–S59; HRESIMS  $m/z$  519.2563 [ $\text{M} + \text{Na}$ ] $^+$  (calcd. for  $\text{C}_{26}\text{H}_{40}\text{O}_9\text{Na}$ , 519.2565,  $\Delta + 0.3$  ppm).

Virescenoside G (**12**): amorphous solids;  $^1\text{H}$  NMR (700 MHz,  $\text{CD}_3\text{OD}$ )  $\delta$ : 5.80 (1H, dd,  $J = 10.8, 17.5$  Hz, H-15), 5.37 (1H, m, H-7), 4.92 (1H, dd,  $J = 1.6, 17.5$  Hz, H-16b), 4.86 (1H, d,  $J = 3.3$  Hz, H-1'), 4.84 (1H, dd,  $J = 1.6, 10.8$  Hz, H-16a), 4.30 (1H, t,  $J = 3.5$  Hz, H-4'), 4.24 (1H, d,  $J = 3.7$  Hz, H-5'), 4.10 (1H, d,  $J = 9.9$  Hz, H-19b), 3.93 (1H, dd,  $J = 3.3, 8.7$  Hz, H-3'), 3.84 (1H, d,  $J = 9.9$  Hz, H-19a), 3.78 (1H, dd,  $J = 3.3, 8.7$  Hz, H-2'), 3.24 (1H, dd,  $J = 4.0, 11.8$  Hz, H-3), 2.07 (1H, m, H-6 $\alpha$ ), 2.01 (1H, m, H-6 $\beta$ ), 1.97 (1H, m, H-14 $\alpha$ ), 1.91 (1H, dd,  $J = 2.7, 14.0$  Hz, H-14 $\beta$ ), 1.90 (1H, dd,  $J = 3.4, 13.4$  Hz, H-1 $\beta$ ), 1.74 (1H, dd,  $J = 3.5, 11.8$  Hz, H-2 $\beta$ ), 1.68 (1H, dd,  $J = 3.5, 7.5$  Hz, H-2 $\alpha$ ), 1.66 (1H, dd,  $J = 3.7, 7.7$  Hz, H-9), 1.57 (1H, m, H-11 $\alpha$ ), 1.47 (1H, td,  $J = 2.9, 9.1$  Hz, H-12 $\beta$ ), 1.37 (1H, m, H-12 $\alpha$ ), 1.38 (1H, m, H-11 $\beta$ ), 1.26 (1H, dd,  $J = 4.5, 12.1$  Hz, H-5), 1.23 (1H, m, H-1 $\alpha$ ), 1.12 (3H, s, Me-18), 0.86 (3H, s, Me-17), 0.85 (3H, s, Me-20).  $^{13}\text{C}$  NMR (176 MHz,  $\text{CD}_3\text{OD}$ )  $\delta$ : 173.7 (C-6'), 152.0 (C-15), 137.1 (C-8), 123.2 (C-7), 110.4 (C-16), 103.9 (C-1'), 81.7 (C-3), 76.7 (C-5'), 73.9 (C-19), 70.6 (C-4'), 70.4 (C-3'), 70.1 (C-2'), 54.1 (C-9), 53.7 (C-5), 47.7 (C-14), 43.7 (C-4), 40.0 (C-1), 38.4 (C-13), 37.9 (C-12), 36.8 (C-10), 29.4 (C-2), 25.0 (C-6), 23.6 (C-18), 22.6 (C-17), 22.1 (C-11), 17.0 (C-20); Supplementary Figures S60–S64; HRESIMS  $m/z$  503.2617 [ $\text{M} + \text{Na}$ ] $^+$  (calcd. for  $\text{C}_{26}\text{H}_{40}\text{O}_8\text{Na}$ , 503.2615,  $\Delta - 0.3$  ppm).

Lactone of virescenoside G (**13**): amorphous solids;  $^1\text{H}$  NMR (700 MHz,  $\text{DMSO}-d_6$ )  $\delta$ : 5.80 (1H, dd,  $J = 10.8, 17.6$  Hz, H-15), 5.66 (1H, d,  $J = 7.8$  Hz, 5'-OH), 5.56 (1H, d,  $J = 5.6$  Hz, 2'-OH), 5.37 (1H, m, H-7), 5.29 (1H, d,  $J = 3.4$  Hz, 2'-OH), 4.93 (1H, dd,  $J = 1.7, 17.6$  Hz, H-16b), 4.85 (1H, dd,  $J = 1.7, 10.7$  Hz, H-16a), 4.68 (1H, d,  $J = 6.8$  Hz, H-1'), 4.41 (1H, dd,  $J = 5.6, 7.8$  Hz, H-5'), 4.39 (1H, brs, H-3'), 4.14 (1H, d,  $J = 11.0$  Hz, H-19b), 4.12 (1H, dd,  $J = 3.4, 5.8$  Hz, H-4'), 3.55 (1H, ddd,  $J = 1.5, 5.4, 6.8$  Hz, H-2'), 3.49 (1H, dd,  $J = 4.0, 11.9$  Hz, H-3), 3.48 (1H, d,  $J = 11.0$  Hz, H-19a), 2.22 (1H, dd,  $J = 3.1, 12.4$  Hz, H-2b), 1.93 (1H, m, H-6 $\beta$ ), 1.91 (1H, m, H-14 $\alpha$ ), 1.88 (1H, m, H-1 $\beta$ ), 1.87 (1H, m, H-14 $\beta$ ), 1.71 (1H, m, H-6 $\alpha$ ), 1.64 (1H, m, H-9), 1.55 (1H, m, H-11b), 1.46 (1H, m, H-2a), 1.44 (1H, m, H-12b), 1.31 (2H, m, H-11a, H-12a), 1.25 (3H, s, Me-18), 1.22 (1H, dd,  $J = 2.5, 9.3$  Hz, H-5), 1.12 (1H, dt,  $J = 3.1, 12.5$  Hz, H-1 $\alpha$ ), 0.89 (3H, s, Me-20), 0.82 (3H, s, Me-17).  $^{13}\text{C}$  NMR (176 MHz,  $\text{DMSO}-d_6$ )  $\delta$ : 174.0 (C-6'), 149.9 (C-15), 135.5 (C-8), 121.1 (C-7), 109.8 (C-16), 93.8 (C-1'), 84.0 (C-3'), 80.1 (C-3), 71.4 (C-2'), 70.1 (C-4'), 68.5 (C-5'), 68.4 (C-19), 50.8 (C-9), 49.9 (C-5), 45.4 (C-14), 36.5 (C-13), 36.1 (C-4), 35.9 (C-1), 35.5 (C-12), 34.7 (C-10), 25.5 (C-18), 21.7 (C-6), 21.3 (C-17), 21.2 (C-2), 19.7 (C-11), 15.7 (C-20); Supplementary Figures S65–S68; HRESIMS  $m/z$  485.2508 [ $\text{M} + \text{Na}$ ] $^+$  (calcd. for  $\text{C}_{26}\text{H}_{38}\text{O}_7\text{Na}$ , 485.2510,  $\Delta + 0.4$  ppm).

Aglycon of virescenoside A (**14**): amorphous solids;  $^1\text{H}$  NMR (500 MHz,  $\text{CD}_3\text{OD}$ )  $\delta$ : 5.80 (1H, dd,  $J = 10.8, 17.5$  Hz, H-15), 5.37 (1H, brs, H-7), 4.93 (1H, dd,  $J = 1.4, 17.5$  Hz, H-16b), 4.85 (1H, dd,  $J = 1.4, 10.8$  Hz, H-16a), 4.14 (1H, d,  $J = 11.2$  Hz, H-19b), 3.79 (1H, ddd,  $J = 4.3, 9.8, 11.7$  Hz, H-2), 3.50 (1H, d,  $J = 11.2$  Hz, H-19a), 3.09 (1H, d,  $J = 9.8$  Hz, H-3), 2.11 (1H, dd,  $J = 4.3, 12.6$  Hz, H-1 $\beta$ ), 1.98 (1H, m, H-6 $\beta$ ), 1.97 (1H, m, H-14 $\alpha$ ), 1.91 (1H, dd,  $J = 2.2, 13.7$  Hz, H-14 $\beta$ ), 1.92 (1H, m, H-6 $\alpha$ ), 1.73 (1H, m, H-9), 1.61 (1H, dt,  $J = 3.9, 10.0$  Hz, H-11 $\beta$ ), 1.50 (1H, d,  $J = 8.7$  Hz, H-12 $\alpha$ ), 1.39 (2H, m, H-11 $\alpha$ , H-12 $\beta$ ), 1.35 (1H, dd,  $J = 4.2, 12.0$  Hz, H-5), 1.21 (3H, s, Me-18), 1.12 (1H, t,  $J = 12.3$  Hz, H-1 $\alpha$ ), 0.93 (3H, s, Me-20), 0.86 (3H, s, Me-17).  $^{13}\text{C}$  NMR (125 MHz,  $\text{CD}_3\text{OD}$ )  $\delta$ : 151.9 (C-15), 137.1 (C-8), 123.1 (C-7), 110.4 (C-16), 86.5 (C-3), 69.7 (C-2), 66.6 (C-19), 54.0 (C-9), 53.0 (C-5), 47.7 (C-1), 47.6 (C-14), 44.4 (C-4), 38.4 (C-13), 37.9

(C-10), 37.8 (C-12), 24.8 (C-6), 24.5 (C-18), 22.6 (C-17), 22.1 (C-11), 17.9 (C-20), Supplementary Figures S69–S73; HRESIMS  $m/z$  343.2241  $[M + Na]^+$  (calcd. for  $C_{20}H_{32}O_3Na$ , 343.2244,  $\Delta + 0.8$  ppm).

### 3.5. Urease Inhibition Assay

The reaction mixture consisting of 25  $\mu$ L enzyme solution (urease from *Canavalia ensiformis*, Sigma, 1U final concentration) and 5  $\mu$ L of test compounds dissolved in water (10–300.0  $\mu$ M final concentration) was preincubated at 37 °C for 60 min in 96-well plates. Then 55  $\mu$ L of phosphate buffer solution with 100  $\mu$ M urea was added to each well and incubated at 37 °C for 10 min. The urease inhibitory activity was estimated by determining of ammonia production using indophenol method [26]. Briefly, 45  $\mu$ L of phenol reagent (1% w/v phenol and 0.005% w/v sodium nitroprusside) and 70  $\mu$ L of alkali reagent (0.5% w/v NaOH and 0.1% active chloride NaOCl) were added to each well. The absorbance was measured after 50 min at 630 nm using a microplate reader Multiskan FC (Thermo Scientific, Canada). All the reactions were performed in triplicate in a final volume of 200  $\mu$ L. The pH was maintained 7.3–7.5 in all assays. DMSO 5% was used as a positive control.

### 3.6. Reactive Oxygen Species (ROS) Level Analysis in LPS-Treated Cells

The suspension of macrophages on 96-well plates ( $2 \times 10^4$  cells/well) were washed with the PBS and treated with 180  $\mu$ L/well of the tested compounds (10  $\mu$ M) for 1 h and 20  $\mu$ L/well LPS from *E. coli* serotype 055:B5 (Sigma, 1.0  $\mu$ g/mL), which were both dissolved in PBS and cultured at 37 °C in a CO<sub>2</sub>-incubator for one hour. For the ROS levels measurement, 200  $\mu$ L of 2,7-dichlorodihydrofluorescein diacetate (DCF-DA, Sigma, final concentration 10  $\mu$ M) fresh solution was added to each well, and the plates were incubated for 30 min at 37 °C. The intensity of DCF-DA fluorescence was measured at  $\lambda_{ex}$  485 nm/ $\lambda_{em}$  518 nm using the plate reader PHERAstar FS (BMG Labtech, Offenburg, Germany) [27].

### 3.7. Reactive Nitrogen Species (RNS) Level Analysis in LPS-Treated Cells

The suspension of macrophages on 96-well plates ( $2 \times 10^4$  cells/well) were washed with the PBS and treated with 180  $\mu$ L/well of the tested compounds (10  $\mu$ M) for 1 h and 20  $\mu$ L/well LPS from *E. coli* serotype 055:B5 (Sigma, 1.0  $\mu$ g/mL), which were both dissolved in PBS and cultured at 37 °C in a CO<sub>2</sub>-incubator for one hour. For the RNS levels measurement, 200  $\mu$ L Diaminofluorescein-FM diacetate (DAF FM-DA, Sigma, final concentration 10  $\mu$ M) fresh solution was added to each well, and the plates were incubated for 40 min at 37 °C, then replaced with fresh PBS, and then incubated for an additional 30 min to allow complete de-esterification of the intracellular diacetates. The intensity of DAF FM-DA fluorescence was measured at  $\lambda_{ex}$  485 nm/ $\lambda_{em}$  520 nm using the plate reader PHERAstar FS (BMG Labtech, Offenburg, Germany).

### 3.8. Peritoneal Macrophage Isolation

Mice BALB/c were sacrificed by cervical dislocation. Peritoneal macrophages were isolated using standard procedures. For this purpose, 3 mL of PBS (pH 7.4) was injected into the peritoneal cavity and the body intensively palpated for 1–2 min. Then the peritoneal fluid was aspirated with a syringe. Mouse peritoneal macrophage suspension was applied to a 96-well plate left at 37 °C in an incubator for 2 h to facilitate attachment of peritoneal macrophages to the plate. Then a cell monolayer was triply flushed with PBS (pH 7.4) for deleting attendant lymphocytes, fibroblasts and erythrocytes and cells were used for further analysis.

All animal experiments were conducted in compliance with all rules and international recommendations of the European Convention for the Protection of Vertebrate Animals used for experimental and other scientific purposes. All procedures were approved by the Animal Ethics Committee at the G. B. Elyakov Pacific Institute of Bioorganic Chemistry, Far Eastern Branch of the Russian Academy of Sciences (Vladivostok, Russia), according to the Laboratory Animal Welfare guidelines.

### 3.9. Statistical Analysis

Average value, standard error, standard deviation and p-values in all experiments were calculated and plotted on the chart using SigmaPlot 3.02 (Jandel Scientific, San Rafael, CA, USA). Statistical difference was evaluated by t-test, and results were considered as statistically significant at  $p < 0.05$ .

## 4. Conclusions

Ten new diterpene glycosides, virescenosides Z<sub>9</sub>-Z<sub>18</sub> (1-10) were isolated from a marine strain of *Acremonium striatisporum* KMM 4401 associated with the holothurian *Eupentacta fraudatrix*. Virescenoside Z<sub>9</sub> (1) is an altroside of a new 7-oxo-isopimara-15-en-2 $\alpha$ ,3 $\beta$ ,6 $\alpha$ ,8 $\beta$ -tetraol aglycon. Virescenosides Z<sub>12</sub>-Z<sub>16</sub> (4-8) were determined as the monosides having unique methyl esters of altruronic acid as their sugar moieties. Carbohydrate chain of virescenoside Z<sub>18</sub> (10) was structurally identified as the methyl ester of mannuronic acid. The effects of some isolated glycosides and aglycons 15-18 on urease activity and regulation of ROS and NO production in macrophages stimulated with lipopolysaccharide (LPC) were evaluated.

**Supplementary Materials:** <sup>1</sup>H, <sup>13</sup>C, HSQC, HMBC and NOESY spectra of all compounds are available online at <http://www.mdpi.com/1660-3397/17/11/616/s1>.

**Author Contributions:** O.I.Z. supervised research, analyzed of NMR spectra and wrote the manuscript; S.S.A. conceptualization, analyzed of NMR spectra and wrote the manuscript; A.S.A. and G.K.O. investigation; Y.V.K. cultivated the fungus; R.S.P. performed MS experiments; V.A.D. performed NMR experiments; E.A.P. evaluated inhibitory effects on ROS and NO production; E.A.C. examined urease activity.

**Funding:** The study was supported by Russian Science Foundation (grant No 19-74-10014).

**Acknowledgments:** The study was carried out on the equipment of the Collective Facilities Center “The Far Eastern Center for Structural Molecular Research (NMR/MS) PIBOC FEB RAS”. The study was carried out using the Collective Facilities Center “Collection of Marine Microorganisms PIBOC FEB RAS”.

**Conflicts of Interest:** The authors declare no conflict of interest.

## References

1. Du, F.Y.; Li, X.M.; Song, J.Y.; Li, C.S.; Wang, B.G. Anthraquinone derivatives and an orsellinic acid ester from the marine alga-derived endophytic fungus *Eurotium cristatum* EN-220. *Helv. Chim. Acta* **2014**, *97*, 973–978. [[CrossRef](#)]
2. Li, D.L.; Li, X.M.; Wang, B.G. Natural anthraquinone derivatives from a marine mangrove plant-derived endophytic fungus *Eurotium rubrum*: Structural elucidation and DPPH radical scavenging activity. *J. Microbiol. Biotechnol.* **2009**, *19*, 675–678.
3. Li, Y.; Li, X.; Lee, U.; Kang, J.S.; Choi, H.D.; Son, B.W. A new radical scavenging anthracene glycoside, asperflavin ribofuranoside, and polyketides from a marine isolate of the fungus *Microsporium*. *Chem. Pharm. Bull.* **2006**, *54*, 882–883. [[CrossRef](#)]
4. Li, X.F.; Xia, Z.Y.; Tang, J.Q.; Wu, J.H.; Tong, J.; Li, M.J.; Ju, J.H.; Chen, H.R.; Wang, L.Y. Identification and biological evaluation of secondary metabolites from marine derived fungi—*Aspergillus* sp. SCSIW3, cultivated in the presence of epigenetic modifying agents. *Molecules* **2017**, *22*, 1302. [[CrossRef](#)] [[PubMed](#)]
5. Wang, Y.N.; Mou, Y.H.; Dong, Y.; Wu, Y.; Liu, B.Y.; Bai, J.; Yan, D.J.; Zhang, L.; Feng, D.Q.; Pei, Y.H.; et al. Diphenyl ethers from a marine-derived *Aspergillus sydowii*. *Mar. Drugs* **2018**, *16*, 451. [[CrossRef](#)] [[PubMed](#)]
6. Hu, Z.X.; Xue, Y.B.; Bi, X.B.; Zhang, J.W.; Luo, Z.W.; Li, X.N.; Yao, G.M.; Wang, J.P.; Zhang, Y.H. Five new secondary metabolites produced by a marine-associated fungus, *Daldinia eschscholzii*. *Mar. Drugs* **2014**, *12*, 5563–5575. [[CrossRef](#)] [[PubMed](#)]
7. Du, L.; Zhu, T.J.; Liu, H.B.; Fang, Y.C.; Zhu, W.M.; Gu, Q.Q. Cytotoxic polyketides from a marine-derived fungus *Aspergillus glaucus*. *J. Nat. Prod.* **2008**, *71*, 1837–1842. [[CrossRef](#)]
8. Harms, H.; Kehraus, S.; Nesaee-Mosaferan, D.; Hufendieck, P.; Meijer, L.; König, G.M. A beta-42 lowering agents from the marine-derived fungus *Dichotomomyces cejpuii*. *Steroids* **2015**, *104*, 182–188. [[CrossRef](#)]

9. Nazir, M.; Harms, H.; Loef, I.; Kehraus, S.; El Maddah, F.; Arslan, I.; Rempel, V.; Muller, C.E.; Konig, G.M. GPR18 inhibiting amaumomine and the novel triterpene glycoside auxarthonoside from the sponge-derived fungus *Auxarthron reticulatum*. *Planta Med.* **2015**, *81*, 1141–1145. [[CrossRef](#)]
10. Afiyatullo, S.S.; Pivkin, M.V.; Kalinovskiy, A.I.; Kuznetsova, T.A. New cytotoxic glycosides of the fungus *Acremonium striatisporum* isolated from a sea cucumber. *Nat. Prod. I* **2007**, *15*, 85–114.
11. Afiyatullo, S.S.; Kalinovskiy, A.I.; Antonov, A.S.; Zhuravleva, O.I.; Khudyakova, Y.V.; Aminin, D.L.; Yurchenko, A.N.; Pivkin, M.V. Isolation and structures of virescenosides from the marine-derived fungus *Acremonium striatisporum*. *Phytochem. Lett.* **2016**, *15*, 66–71. [[CrossRef](#)]
12. Afiyatullo, S.S.; Kalinovskiy, A.I.; Antonov, A.S. New virescenosides from the marine-derived fungus *Acremonium striatisporum*. *Nat. Prod. Commun.* **2011**, *6*, 1063–1068. [[CrossRef](#)] [[PubMed](#)]
13. Polonsky, J.; Baskevitch, Z.; Cagnoli-Bellavita, N.; Ceccherelli, P. Structures des virescenols A et B, metabolites de *Oospora virescens* (link) Wallr. *Tetrahedron* **1970**, *29*, 449–454.
14. Polonsky, J.; Baskevitch, Z.; Cagnoli-Bellavita, N.; Ceccherelli, P.; Buckwalter, B.L.; Wenkert, E. Carbon-13 nuclear magnetic resonance spectroscopy of naturally occurring substances. XI. Biosynthesis of virescenosides. *J. Am. Chem. Soc.* **1972**, *94*, 4369–4370. [[CrossRef](#)]
15. Wenkert, E.; Beak, P. The stereochemistry of rumiene. *J. Am. Chem. Soc.* **1961**, *83*, 998–1000. [[CrossRef](#)]
16. De Pascual, J.T.; Barrero, A.F.; Muriel, L.; San Feliciano, A.; Grande, M. New natural diterpene acid from *Juniperus communis*. *Phytochemistry* **1980**, *19*, 1153–1156. [[CrossRef](#)]
17. Afiyatullo, S.S.; Kalinovskiy, A.I.; Kuznetsova, T.A.; Isakov, V.V.; Pivkin, M.V.; Dmitrenok, P.S.; Elyakov, G.B. New diterpene glycosides of the fungus *Acremonium striatisporum* isolated from a sea cucumber. *J. Nat. Prod.* **2002**, *65*, 641–644. [[CrossRef](#)]
18. Afiyatullo, S.S.; Kuznetsova, T.A.; Isakov, V.V.; Pivkin, M.V.; Prokof'eva, N.G.; Elyakov, G.B. New diterpenic altrosides of the fungus *Acremonium striatisporum* isolated from a sea cucumber. *J. Nat. Prod.* **2000**, *63*, 848–850. [[CrossRef](#)]
19. Ceccherelli, P.; Cagnoli-Bellavita, N.; Polonsky, J.; Baskevitch, Z. Structures des virescenosides F et G, nouveaux metabolites de *Oospora virescens* (link) Wallr. *Tetrahedron* **1973**, *29*, 449–454. [[CrossRef](#)]
20. Bellavita, N.; Bernassau, J.-M.; Ceccherelli, P.; Raju, M.S.; Wenkert, E. An unusual solvent dependence of the carbone-13 nuclear magnetic resonance spectral features of some glycosides as studied by relaxation-time measurements. *J. Am. Chem. Soc.* **1980**, *2*, 17–20. [[CrossRef](#)]
21. Afiyatullo, S.S.; Kalinovskiy, A.I.; Pivkin, M.V.; Dmitrenok, P.S.; Kuznetsova, T.A. New diterpene glycosides of the fungus *Acremonium striatisporum* isolated from a sea cucumber. *Nat. Prod. Res.* **2006**, *20*, 902–908. [[CrossRef](#)] [[PubMed](#)]
22. King-Morris, M.J.; Serrianni, A.S. <sup>13</sup>C NMR studies of [1-<sup>13</sup>C] aldoses: Empirical rules correlating pyranose ring configuration and conformation with <sup>13</sup>C chemical shifts and <sup>13</sup>C-<sup>13</sup>C spin couplings. *J. Am. Chem. Soc.* **1987**, *109*, 3501–3508. [[CrossRef](#)]
23. Podlasek, C.A.; Wu, J.; Stripe, W.A.; Bondo, P.B.; Serrianni, A.S. [<sup>13</sup>C]-Enriched methyl aldopyranosides: Structural interpretations of <sup>13</sup>C-<sup>1</sup>H spin-coupling constants and <sup>1</sup>H chemical shifts. *J. Am. Chem. Soc.* **1995**, *117*, 8635–8644. [[CrossRef](#)]
24. Burne, R.A.; Chen, Y.Y. Bacterial ureases in infectious diseases. *Microbes Infect.* **2000**, *2*, 533–542. [[CrossRef](#)]
25. Mobley, H.L.; Hausinger, R.P. Microbial ureases: Significance, regulation, and molecular characterization. *Microbiol. Rev.* **1989**, *53*, 85–108.
26. Weatherburn, M.W. Phenol hypochlorite reaction for determination of ammonia. *Anal. Chem.* **1967**, *39*, 971–974. [[CrossRef](#)]
27. Ivanchina, N.V.; Kicha, A.A.; Malyarenko, T.V.; Kalinovskiy, A.I.; Menchinskaya, E.S.; Pisyagin, E.A.; Dmitrenok, P.S. The influence on LPS-induced ROS formation in macrophages of capelloside A, a new steroid glycoside from the starfish *Ogmaster capella*. *Nat. Prod. Commun.* **2015**, *10*, 1937–1940. [[CrossRef](#)]

